Available online at www.sciencedirect.com
SCIENCE DIRECT®
International Journal of Heat and Mass Transfer 49 (2006) 3401–3407
International Journal of HEAT and MASS TRANSFER
www.elsevier.com/locate/ijhmt

Molecular dynamics simulations of heat and momentum transfer at a solid–fluid interface: Relationship between thermal and velocity slip

Rajesh Khare [a,1], Pawel Keblinski [b,*], Arun Yethiraj [c]

[a] Department of Chemical and Biological Engineering, University of Wisconsin – Madison, 1415 Engineering Dr., Madison, WI 53706, USA
[b] Materials Science and Engineering Department, Rensselaer Polytechnic Institute, 110 8th St., MRC 115, Troy, NY 12180, USA
[c] Department of Chemistry, University of Wisconsin – Madison, 8305b Chemistry Bldg, 1101 University Ave., Madison, WI 53706, USA

Received 6 August 2005; received in revised form 24 February 2006
Available online 11 May 2006

Abstract

The thermal resistance of a model solid–liquid interface in the presence of laminar shear flow is investigated using molecular dynamics simulations. Two model liquids – a monoatomic liquid and a polymeric liquid composed of 20 repeat units – are confined between walls which are modeled as idealized lattice surfaces composed of atoms identical to the monomers. We find that in the absence of a velocity slip (discontinuity) at the solid–fluid interface, the mass flow does not affect the thermal interfacial resistance, but the presence of velocity slip results in an increase in the interfacial thermal resistance by about a factor of two.

Keywords: Interfacial thermal resistance; Velocity slip; Molecular dynamics

1. Introduction

A description of heat flow at the macroscopic level involves two inputs: (i) a constitutive relation between heat fluxes and driving forces, e.g., temperature gradients, and (ii) boundary conditions at the system perimeter. For example, in the absence of mass flow, one constitutive relation between the thermal energy flux, $\mathbf{j}_Q$ and the temperature gradient is Fourier's law:

$$\mathbf{j}_Q = -\lambda \nabla T, \tag{1}$$

where λ is the material bulk thermal conductivity. In the absence of internal heat sources, conservation of energy enables us to write a second order partial differential equation for the diffusive heat flow, which can be solved for the temperature profile as a function of spatial and temporal variables if appropriate boundary conditions are available. Conservation of energy requires that the thermal flux be continuous at the boundary. It is often assumed that the temperature is also continuous at the boundary.

In this work we investigate the boundary conditions for heat flow using molecular dynamics simulations. We are particularly interested in the behavior of the temperature profile at the boundary. Fluids undergoing shear flow often display velocity slip at the surface, i.e., the velocity of the fluid extrapolated to the surface position is different from the surface velocity. In an analogous fashion, it is possible for the extrapolated temperature of the fluid to be different from the surface temperature. This is the result of an interfacial thermal resistance that can have a significant effect on the thermal transport in fluids, particularly in nanofluidic systems. Computer simulations can provide molecular insight into the origin and mechanism of such interfacial thermal behavior.

Although it is often assumed that the temperature is continuous across an interface, in reality there is no

* Corresponding author. Tel.: +1 518 276 6858; fax: +1 518 276 8554.
E-mail addresses: rajesh.khare@ttu.edu (R. Khare), keblip@rpi.edu (P. Keblinski).
[1] Present address: Department of Chemical Engineering, Texas Tech University, P.O. Box 43121, Lubbock, TX 79409-3121, USA.

0017-9310/$ - see front matter © 2006 Elsevier Ltd. All rights reserved.
doi:10.1016/j.ijheatmasstransfer.2006.03.005

Nomenclature

$\mathbf{j}_Q$	thermal flux
k_B	Boltzmann constant
l_K	Kapitza length
m	mass of an atom (bead)
r	distance between two atoms
R_K	interfacial thermal resistance (Kapitza resistance)
v_x	x component of shear velocity
T	temperature

Greek symbols

δ	slip length
ε	Lennard-Jones potential energy parameter
λ	thermal conductivity
Λ	interfacial thermal conductance
ρ	density
σ	Lennard-Jones potential length parameter
τ	Lennard-Jones reduced time unit, $\tau = \sigma\sqrt{m/\varepsilon}$

firm physical basis for this assumption. In fact, Kapitza [1,2] demonstrated the possibility of a discontinuous temperature drop at an interface. This drop is quantified by the concept of interfacial conductance, Λ, which is the ratio of the heat flux (in the direction normal to interface) to the temperature drop. The inverse of Λ is the interfacial thermal resistance, also called the Kapitza resistance, R_K.

The Kapitza resistance is not significant for most solid–liquid interfaces, but can be significant in nano-structured materials. To estimate the significance of the Kapitza resistance, one can express it in terms of the "thermal resistance thickness", l_K, also called the Kapitza length, which is defined as the width of the bulk medium over which there would be the same temperature drop as that at the interface. The Kapitza length is therefore given by

$$l_K = \frac{\lambda}{\Lambda} = R_K \lambda. \tag{2}$$

Typically, in the case of a solid–liquid interface involving a wetting liquid, Kapitza length is of the order of a molecular size and thus the temperature drop at the interfaces can be neglected. However, for non-wetting liquids [3,4], l_K can be of the order of several tens of molecular sizes. In this case, the interfacial resistance might impact the thermal transport in fluids, particularly in structures involving nanoscale dimensions, such as nanofluids. Other systems where the boundary resistance plays an important role are polycrystalline high thermal conductivity materials, such as diamond [5], where grain boundaries lead to large values of l_K, despite relatively low values of R_K, because the bulk thermal conductivity is high.

The Kapitza length plays the same role in heat transfer as the slip length in momentum transfer. When a fluid is sheared by a confining surface the boundary conditions can be either stick or slip. In the latter case, the slip length, δ, describes the discontinuity of the velocity field (velocity component tangential to the solid–liquid interface) at the surface [4]. In planar shear flow geometry δ can be evaluated from

$$\delta = \Delta v_x(z=0) \Big/ \left(\frac{\mathrm{d}v_x}{\mathrm{d}z}\right)_{z=0}, \tag{3}$$

where the fluid flow direction is in the x direction, the z direction is normal to the fluid–solid interface and $\Delta v_x(z=0)$ is the velocity discontinuity at the interface. In the case of a stick boundary condition, the velocity field is continuous at the interface, and therefore $\Delta v_x(z=0) = 0$ and $\delta = 0$. In the case of slip, δ has a geometrical interpretation of a distance to which a linear v_x vs. z velocity profile has to be extrapolated (beyond the solid–fluid interface) to recover the same value of velocity as the solid surface velocity. For atomistically smooth solid surfaces and especially for systems showing weak interfacial bonding characteristics, both modeling and experimental studies have demonstrated a possibility of δ reaching values of several tens of molecular sizes [6–11]. The effects of non-zero values of δ become important when the characteristic fluid channel sizes are reduced to submicron or nanoscale dimensions.

The Kaptiza length can be defined in an analogous fashion in terms of the temperature drop at the interface and the temperature gradient in the liquid at the interface, i.e.,

$$l_K = \Delta T(z=0) \Big/ \left(\frac{\mathrm{d}T}{\mathrm{d}z}\right)_{z=0}, \tag{4}$$

which allows one to calculate l_K without knowledge of the absolute values of the thermal conductivity or the interfacial thermal conductance.

The primary goal of this work is to elucidate the relationship between the velocity slip and thermal slip. While there have been many studies that have addressed the slip length [6–11] or the Kapitza length [1–4,12] (for systems undergoing pure thermal transport), we are not aware of any study that focuses on the possible relationship between the velocity slip and the thermal slip. To address this question, we perform a series of molecular dynamics simulations of thermal transport across solid–liquid interfaces for stationary liquids and for liquids subjected to a planar shear flow.

We report results on molecular dynamics simulations of monatomic and polymeric fluids confined between atomistically smooth surfaces, with Lennard-Jones interactions between all sites. We compare the results for the slip length and Kapitza length in three cases: (i) where the fluid is subjected to planar shear flow with the walls held at constant

temperature, (ii) where the walls are at the same temperature as in (i) but instead of shear flow, heat is artificially pumped into the liquid, and (iii) where there is no shear flow but a temperature gradient is imposed across the fluid by maintaining the walls at different temperatures. We find that when there is no velocity slip, shear flow does not affect the value of the Kapitza length, but a large slip in the velocity profile causes an increase of l_K by about a factor of 2. We therefore conclude that the slip length and Kapitza length are interdependent quantities.

The rest of the paper is organized as follows. The simulation model and the methods are described in Section 2, simulation results are presented and discussed in Section 3, and some conclusions are presented in Section 4.

2. Simulation method

Two types of liquids are studied: simple monatomic liquids and polymeric liquids (chain length = 20) that are modeled using a bead-spring representation. In both cases, all beads interact with a pairwise additive Lennard-Jones (LJ) potential:

$$U(r)^{\mathrm{LJ}} = 4\varepsilon\left[\left(\frac{\sigma}{r}\right)^{12} - \left(\frac{\sigma}{r}\right)^{6}\right], \tag{5}$$

where the LJ parameter σ sets the length scale (~molecular size) and ε defines the energy scale. The fluid structure near the confining walls and hence the flow boundary conditions (slip/no-slip) can be altered by altering the strength of the interaction potential between the fluid atoms and the wall atoms [13,14]. To capture this effect, we use two types of LJ potential based interactions. The first is the so called WCA potential [15] (or a purely repulsive Lennard-Jones potential) where the potential is truncated at its minimum $r = 2^{1/6}\sigma$, and a regular Lennard Jones potential truncated at $r = 2.5\sigma$. In both cases the potential is shifted so that it is a continuous function.

Adjacent beads of the chains are connected by FENE springs [16] with a potential given by

$$U(r)^{\mathrm{FENE}} = -\frac{HQ^2}{2}\ln\left[1 - \left(\frac{r}{Q}\right)^2\right]. \tag{6}$$

Following our previous work [17], we use $H = 100\varepsilon/\sigma^2$ and $Q = 1.5\sigma$. The FENE potential along with the LJ potential not only provides chain connectivity but also prevents the polymer chains from crossing each other.

The simulation setup used in our work is depicted in Fig. 1. The liquid is confined between two solid walls that are either at rest or move with the same speed but in opposite directions (in the $+x$ and $-x$ directions). Periodic boundary conditions are employed in the other two directions. The confining surfaces are modeled using idealized, (100) FCC lattice surfaces located at $z = 0$ and $z = 18\sigma$ thus leading to overall simulation box dimensions of $11.7 \times 11.7 \times 18.0$ (in units of σ). In practice, the surfaces consist of beads that are connected to FCC lattice sites

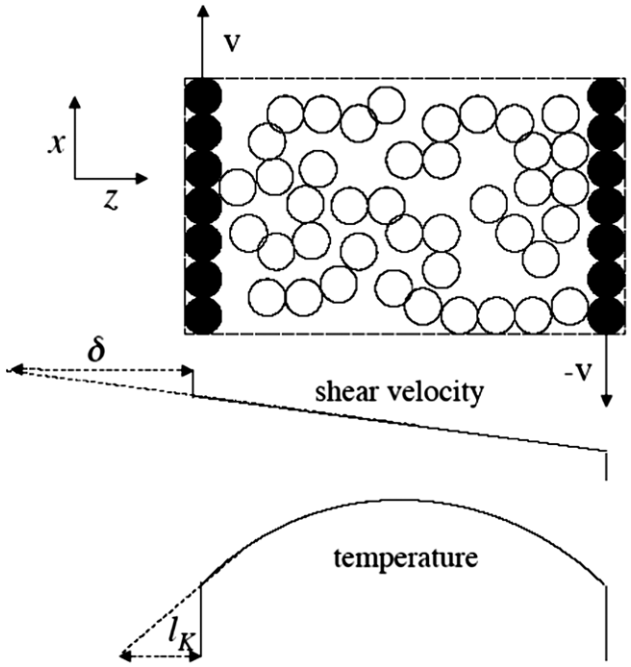

Fig. 1. A sketch of the simulation setup, which also illustrates the concept of the thermal slip via the Kapitza length (l_K) and the velocity slip length (δ).

using harmonic springs with a spring constant of $500\varepsilon/\sigma^2$ [17].

For liquids described by the WCA (LJ) potential, the beads that make up the surface interact with the beads of the liquid via the WCA (LJ) potential. For liquids described by the full LJ potential, the liquid–surface interactions are also described by the full LJ potential but with the energy parameter ε five times larger than for the liquid–liquid interaction, i.e., $\varepsilon_{\mathrm{liquid-solid}} = 5.0\varepsilon_{\mathrm{liquid-liquid}}$. Such a strong attraction between the liquid and the solid atoms corresponds to a strongly wetting liquid and is known to translate into no-slip (no discontinuity) velocity boundary conditions at the liquid–solid interface [14].

Molecular dynamics simulations are carried out using the velocity Verlet algorithm. A MD time step of 0.002 in the reduced LJ time unit ($\tau = \sigma\sqrt{m/\varepsilon}$), is used for evaluating the trajectories of the beads. In all cases, the solid walls are maintained at a specified temperature by coupling them to a heat bath via a Langevin thermostat [18]. The reduced density, $\rho^* = \rho\sigma^3$, for all simulations is 0.8 where ρ is the bead number density (i.e., number of beads per unit volume). The reader is referred to previous work [17,19] for more details on the simulation methods.

In order to investigate the coupling between momentum and heat transfer at the solid–liquid interface, three different types of simulations are carried out:

(i) Momentum transport is studied by simulating planar shear flow of the confined fluid. In this case, shear is imparted on the confined fluid by moving the two walls with the same speed, $v = 1.8\sigma/\tau$, but in opposite

directions along the x axis. As has been noted in previous simulation work [17,19] and by continuum mechanics [20], at sufficiently high shear rates, viscous heating throughout the volume of the liquid raises its temperature. It is to be noted that the shear rates used in the current work might appear to be small in the reduced Lennard-Jones units that are used in this paper (as is customary in the simulation literature). On the other hand, depending on the strategy used for mapping our model chain systems onto real polymers, the actual shear rate values will be very high. Experimentally, viscous dissipation effects are found to be significant only at shear rates much higher than $10^6\ s^{-1}$ for gaps of size of a few microns [21]. This flow-generated heat is removed from the liquid via thermal conduction to the solid walls that are kept at fixed temperature, $k_B T \cong 3\varepsilon$, where k_B is the Boltzmann's constant. In these simulations, a steady state is characterized by a linear velocity profile (with or without slip) and a parabolic temperature profile symmetric about the center of the channel.

(ii) To separate out the effects due to a possible coupling between the momentum and heat transfer, we carry out simulations with no shear flow but with heat artificially "pumped" into the liquid. This is achieved by re-scaling the velocities of all the atoms (at every 5 MD steps) to maintain the average fluid temperature at a given value above the temperature of the confining walls. The average fluid temperature is adjusted (by a process of trial and error) so that the maximum fluid temperature (at the center of the channel) is the same as that observed in the corresponding shear flow simulation (i).

(iii) Standard heat transfer is studied by simulating thermal conduction through the confined fluid in the presence of an imposed temperature gradient. In this case, a temperature gradient is imposed on the system by maintaining the two walls at different temperatures $k_B T \cong 3\varepsilon$ and $k_B T \cong 4\varepsilon$, respectively.

At this point, we would like to make two observations regarding the evaluation of the temperature profile in the system:

(1) For systems with fluid flow, temperature is determined by using the kinetic energy calculated based only on the "peculiar" or the "thermal" part of the atom velocity (which is obtained by subtracting the net local flow velocity from the total velocity of the atoms) [22,23].

(2) As mentioned earlier, the walls consist of a single layer of atoms – this model precludes the possibility of a temperature gradient within the confining solid walls. We consider such a model to be adequate, since a typical solid crystalline material that will constitute the wall, will have a significantly higher thermal conductivity than the fluid, thus leading to absence of any temperature gradient within the solid material.

A typical simulation run consists of three phases: generation of an initial configuration, approach to steady state, and averaging. For the monomeric fluid, initial configuration was obtained by using molecular dynamics to "melt" an initially ordered configuration of the required number of monomers, while for the polymer melt, initial configuration of chains containing 20 beads each was generated using a growth and equilibration algorithm [24]. We first allow for 500,000 MD steps for the system to reach the steady state followed by another 500,000 MD steps for the averaging of properties such as the velocity, temperature, and density profiles, and the chain conformational properties. These profiles are evaluated by dividing the liquid film in the z (normal to the walls) direction into bins of size 0.5σ for the velocity and temperature profiles and bins of size 0.1σ for the density profiles. The averaging phase is divided into 10 blocks and the method of block averaging is used to obtain an estimate of the statistical uncertainties.

3. Results and discussion

Fig. 2 depicts the velocity profiles of two confined monatomic liquids, the first involving only repulsive interactions and the second involving strong attractions between the fluid and the solid walls (i.e., full LJ potential with $\varepsilon_{\text{liquid–solid}} = 5.0\varepsilon_{\text{liquid–liquid}}$). We will refer to these systems as the repulsive and attractive liquids, respectively. It can be seen that even for the repulsive monatomic fluid the velocity slip is quite small (the line depicts a linear fit to the velocity profile in the region $1.5\sigma < z < 16.5\sigma$), with a slip length $\sim 0.6\sigma$. When attractions are included there is no evidence of slip at the solid wall.

Fig. 3 depicts the temperature profiles of the repulsive monatomic liquid subject to planar shear flow and for the case where heat is artificially pumped in the system.

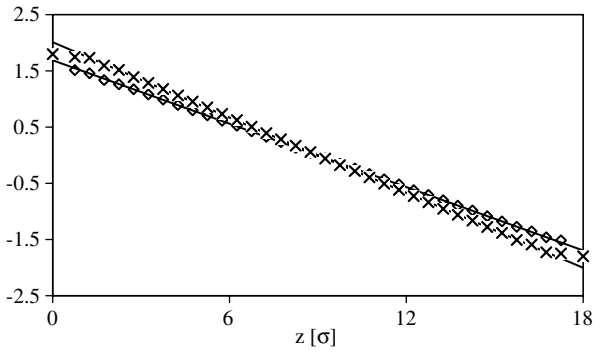

Fig. 2. Velocity profiles of the "repulsive" (diamonds) and "attractive" (crosses) monatomic liquid subject to planar shear flow (wall velocity = 1.8). The straight lines depict linear fits to the velocity profiles in the region $1.5\sigma < z < 16.5\sigma$. The error bars for all velocity profiles reported in this work are about the same size as the size of the symbols used.

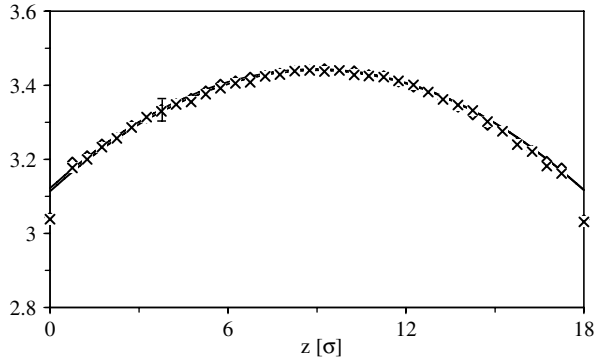

Fig. 3. Temperature profiles of the "repulsive" monatomic liquid with "artificial heat generation" (crosses) and "shear flow" (diamonds) simulations. The curves represent quadratic fits to the temperature profiles in the region $1.5\sigma < z < 16.5\sigma$. A typical error bar for all the temperature profiles reported in this work is also shown.

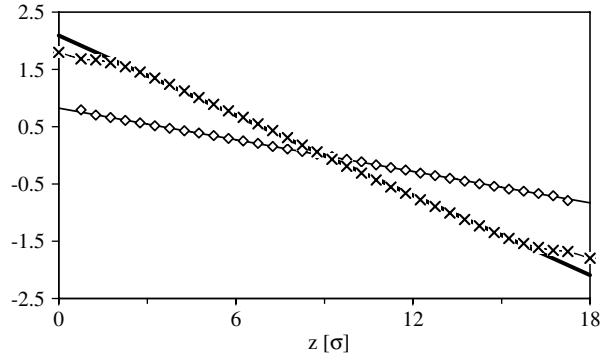

Fig. 4. Velocity profiles of the "repulsive" (diamonds) and "attractive" (crosses) polymer melt subject to planar shear flow (wall velocity = 1.8). The straight lines depict linear fits to the velocity profiles in the region $1.5\sigma < z < 16.5\sigma$.

The temperature profile of the sheared fluid is parabolic with a temperature rise in the middle region compared to near the surfaces. This is a consequence of viscous heating in the fluid. The parabolic shape originates simply from the fact that the heat flux through a given plane is proportional to the distance from the channel center. Since the heat flux is proportional to the temperature gradient, a parabolic temperature profile is obtained upon integration. The figure also shows that there is thermal slip in the repulsive monatomic fluid even in the absence of velocity slip (as was noted in the earlier paragraph). The temperature profiles of the sheared fluid and the fluid with heat artificially pumped (by re-scaling the velocities) are essentially identical (within the error bars), i.e., it does not make a difference whether the heat is generated by viscous heating (due to the movement of the surfaces) or pumped uniformly into the system. By first fitting the temperature profiles in the liquid (in the region $1.5\sigma < z < 16.5\sigma$) to second order polynomials and then calculating ΔT and $\mathrm{d}T/\mathrm{d}z$ extrapolated to the solid wall, we calculate the Kapitza length of the monoatomic repulsive liquid to be 1.1σ.

There are significant differences in the behavior of polymer melts, when compared to monatomic liquids. In the case of repulsive polymer melts, there is significant slip at the surfaces, as has been noted previously [17]. Including wall–fluid attractions greatly decreases the magnitude of this slip. Fig. 4 depicts the velocity profiles for the repulsive and attractive polymer melts (the terms "attractive" and "repulsive" have the same meaning as in the discussion of monatomic liquids). The velocity profile is linear in both cases with the exception of a small region near the walls. The repulsive polymer liquid exhibits a large velocity slip (discontinuity) with a corresponding slip length of 10.6σ. The attractive polymer melt, on the other hand, does not exhibit any slip at the two walls. In fact, for this system, the velocity profile shows a smaller slope in the region near the walls than in the "bulk-like" region in the central part of the channel. This indicates that the strong attraction leads to a layer of the polymer that is effectively bonded to the wall and hence moves with the wall. From the macroscopic point of view, this bonded layer leads to a negative slip length of -1.3σ.

Fig. 5 compares temperature profiles for the sheared "repulsive" polymer melt to the case where heat is artificially pumped into the system. In both cases, the temperature profiles are parabolic and exhibit a maximum at the center of the fluid, and in both cases there is a discontinuity in the temperature profile at the solid liquid interface. Although, by construction, the maximum value of the temperature at the channel center is almost the same, the temperature discontinuity at the solid–liquid interface is larger for the sheared fluid, and the Kapitza lengths for the shear and no shear (heat artificially pumped into the system) cases are $l_K = 3.2\sigma$ and $l_K = 1.5\sigma$, respectively. In other words, the velocity slip associated with the shear flow appears to result in approximate doubling of the thermal resistance and consequently the Kapitza length.

One might speculate that, to some extent, the observed effect of the velocity slip on the thermal slip is due to the very large shear rates used in simulations. To this end,

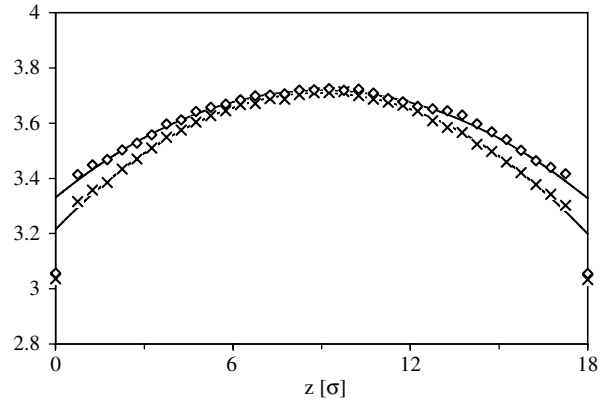

Fig. 5. Temperature profiles of the "repulsive" polymer melt with "artificial heat generation" (crosses) and "shear flow" (diamonds) simulations. The curves represent quadratic fits to the temperature profiles in the region $1.5\sigma < z < 16.5\sigma$.

we checked the effect of the shear rate on our results by simulating the repulsive polymer melt at a shear rate that was half of the value studied above (thus leading to wall velocity $= v = 0.9\sigma/\tau$). These simulations yielded essentially the same result with the approximate doubling of the Kapitza length upon shear induced velocity slip.

Fig. 6 compares temperature profiles for the sheared "attractive" polymer melt to the case where heat is artificially pumped into the system. Except for the immediate vicinity of the surface, the temperature profiles in the two cases are identical within statistical uncertainties, i.e., for the attractive polymeric liquid there is no effect of the shear flow on the interfacial heat transfer. This is in contrast to what is observed for the repulsive polymer liquid. We hypothesize that this is related to the fact that there is no velocity slip at the interface for the attractive polymer liquid, since similar effects are seen in the monatomic fluids. In fact, as was the case for the velocity profile, the temperature gradients are smaller (corresponding to locally higher thermal conductivities) in the interfacial regions ($\sim 2\sigma$ from each wall) than in the channel center. Within the macroscopic picture, this observation translates into a negative Kapitza length of -0.7σ.

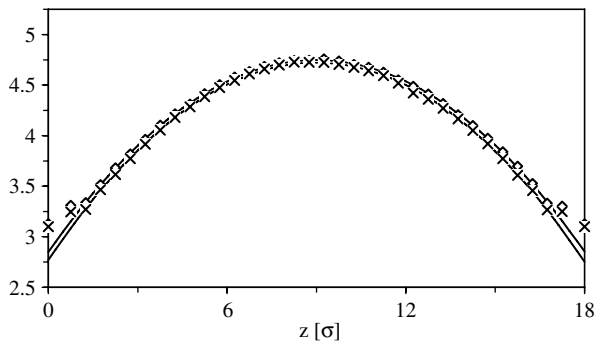

Fig. 6. Temperature profiles of the "attractive" polymer melt with "artificial heat generation" (crosses) and "shear flow" (diamonds) simulations. The curves represent quadratic fits to the temperature profiles in the region $1.5\sigma < z < 16.5\sigma$.

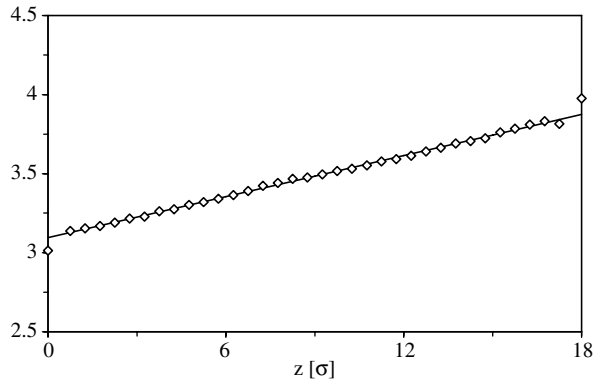

Fig. 7. Temperature profile for the "repulsive" polymeric melt system subject to a thermal gradient. The straight line represents linear fit to the temperature profile in the region: $1.5\sigma < z < 16.5\sigma$.

It is instructive to compare the values of l_K obtained as above to simulations where a temperature gradient is imposed on the fluid externally. Fig. 7 depicts the temperature profile in a standard heat transfer measurement configuration with a stationary repulsive polymeric liquid confined between two walls at different temperatures. At the cold wall (maintained at $k_B T \cong 3\varepsilon$), we find $l_K \cong 1.9\sigma$, in reasonable agreement with the value obtained with the parabolic temperature profile under no-shear condition (see earlier text and Fig. 5). At the hot wall (maintained at $k_B T \cong 4\varepsilon$), we find $l_K \cong 2.3\sigma$, This difference between cold and hot sides indicates a temperature dependence of the Kapitza resistance, since a good linear fit to the temperature profile in Fig. 7 indicates that the liquid thermal conductivity is essentially constant throughout the liquid at these simulation conditions.

4. Conclusions

We present molecular dynamics simulations for the heat and momentum transfer at solid–liquid interfaces. We find that both thermal and velocity slip are strongly influenced by the fluid–wall interactions. Thermal slip is present in sheared liquids even without substantial velocity slip, although the presence of velocity slip enhances the magnitude of thermal slip. We find that at the conditions investigated in this work, the shear flow induces an increase in the Kapitza length for a polymer melt by approximately a factor of two, and this effect on the interfacial heat transfer is observed only when there is a large velocity slip at the solid–liquid interface. Interestingly, the Kapitza length is found to be temperature dependent even when the thermal conductivity of the fluid appears to be approximately constant as a function of temperature.

The dependence of the interfacial thermal resistance on shear flow is probably caused by dynamical rather than structural effects. Previous work has shown that the density profile of liquids is relatively insensitive to shear [17]. In

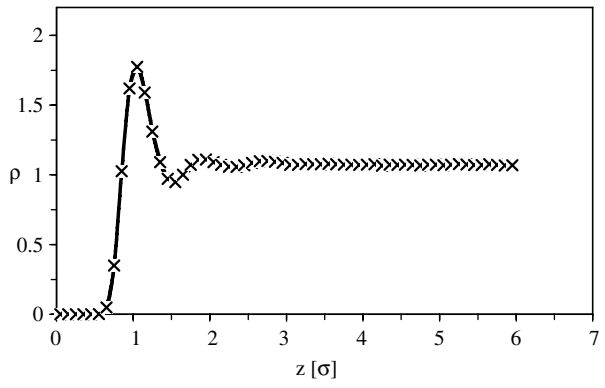

Fig. 8. Bead density profiles as a function of the z coordinate (normal to the walls) for the "repulsive" polymeric melt system. The figure shows density profiles for both the "artificial heat pumping" (crosses) and "shear flow" (solid line) simulations.

our simulations the density profiles of the sheared and static (where heat is artificially pumped into the system) fluids are almost identical (see Fig. 8). Although the shear flow elongates the chains in the shear direction, this effect is modest, about a 10% effect in our simulations. The structural differences between sheared and static polymer melts are therefore quite small. If one thinks of velocity slip as being due to inefficient momentum transfer from the fluid to the surface, one would expect dynamical effects to play a significant role. This work suggests that interfacial heat transfer is closely coupled to interfacial momentum transfer. Further studies aimed at elucidating the precise nature of these dynamical effects would be of considerable interest.

Acknowledgements

RK thanks Profs. Michael Graham and Juan de Pablo for many insightful discussions on the topic of coupled heat and momentum transfer. RK acknowledges National Science Foundation (Grant No. NSF-NSEC DMR-0425880) for partial support of this work. AY acknowledges partial support of this work by the National Science Foundation under Grant No. CHE-0315219. PK was supported by DOE Grant No. DE-FG02-04ER46104.

References

[1] P.L. Kapitza, Zh. Eksp. Theor. Fiz. 11 (1941) 1 [J. Phys. USSR 4, 181].
[2] E.T. Schwartz, R.O. Pohl, Thermal boundary resistance, Rev. Mod. Phys. 61 (1989) 605–689.
[3] L. Xue, P. Keblinski, S.R. Phillpot, S.U.S. Choi, J.A. Eastman, Two regimes of thermal resistance at a liquid–solid interface, J. Chem. Phys. 118 (2003) 337–339.
[4] J.-L. Barrat, F. Chiaruttini, Kapitza resistance at the liquid solid interface, Mol. Phys. 101 (2003) 1605–1610.
[5] J.E. Graebner, S. Jin, G.W. Kammolott, J.A. Herb, F.F. Gardinier, Large anisotropic thermal conductivity in synthetic diamond films, Nature 359 (1992) 401–403.
[6] N.V. Churaev, V.D. Sobolev, A.N. Somov, Slippage of liquids over lyophobic solid-surfaces, J. Colloid Interface Sci. 97 (1984) 574–581.
[7] J. Baudry, A. Tonck, D. Mazuyer, E. Charlaoix, Experimental evidence for a large slip effect at a nonwetting fluid–solid interface, Langmuir 17 (2001) 5232–5236.
[8] C. Cottin-Bizonne, S. Jurine, J. Baudry, J. Crassous, F. Restagno, E. Charlaix, Nanorheology: an investigation of the boundary condition at hydrophobic and hydrophilic interfaces, Eur. Phys. J. E 9 (2002) 47–53.
[9] Y.X. Zhu, S. Granick, Rate-dependent slip of Newtonian liquid at smooth surfaces, Phys. Rev. Lett. 87 (2001) 096105.
[10] M.O. Robbins, M.H. Muser, Computer simulations of friction, lubrication and wear, in: B. Bhushan (Ed.), Modern Tribology Handbook, CRC Press, Boca Raton, FL, 2001, pp. 717–765.
[11] J.-L. Barrat, L. Bocquet, Large slip effect at a nonwetting fluid–solid interface, Phys. Rev. Lett. 82 (1999) 4671–4674.
[12] S. Maruyama, T. Kimura, A study of thermal resistance over a solid–liquid interface by molecular dynamic simulations, Ther. Sci. Eng. 7 (1999) 63–68.
[13] P.A. Thompson, M.O. Robbins, Shear flow near solids: epitaxial order and flow boundary conditions, Phys. Rev. A 41 (1990) 6830–6837.
[14] E. Manias, G. Hadziioannou, I. Bitsanis, G. Ten Brinke, Stick and slip behavior of confined oligomer melts under shear. A molecular-dynamics study, Europhys. Lett. 24 (1993) 99–104.
[15] J.D. Weeks, D. Chandler, H.C. Andersen, Role of repulsive forces in determining equilibrium structure of simple liquids, J. Chem. Phys. 54 (1971) 5237–5247.
[16] G.S. Grest, K. Kremer, Dynamics of entangled linear polymer melts – a molecular dynamics simulation, J. Chem. Phys. 92 (1990) 5057–5086, and references therein.
[17] R. Khare, J.J. de Pablo, A. Yethiraj, Rheology of confined polymer melts, Macromolecules 29 (1996) 7910–7918.
[18] M.P. Allen, D.J. Tildesley, Computer Simulation of Liquids, Oxford University Press, Oxford, 1992.
[19] R. Khare, J.J. de Pablo, A. Yethiraj, Molecular simulation and continuum mechanics study of simple fluids in non-isothermal planar Couette flows, J. Chem. Phys. 107 (1997) 2589–2596.
[20] R.B. Bird, W.E. Stewart, E.N. Lightfoot, Transport Phenomena, John Wiley & Sons, New York, 1960.
[21] H.H. Winter, Viscous dissipation in shear flows of molten polymers, Adv. Heat Transfer 13 (1977) 205.
[22] W. Loose, G. Ciccotti, Temperature and temperature control in nonequilibrium-molecular-dynamics simulations of the shear flow of dense liquids, Phys. Rev. E 45 (1992) 3859–3866.
[23] S.Y. Liem, D. Brown, J.H.R. Clarke, Investigation of the homogeneous-shear nonequilibrium-molecular-dynamics method, Phys. Rev. E 45 (1992) 3706–3713.
[24] A. Yethiraj, C.K. Hall, Monte Carlo simulation of polymers confined between flat plates, Macromolecules 23 (1990) 1865–1872.